Inlet shape optimization of pneumobile engine pneumatic cylinder using CFD analysis

M. Černák, M. Michalec, M. Valena and M. Ranuša

Institute of Machine and Industrial Design, Faculty of Mechanical Engineering, Brno University of Technology, Technická 2, Brno, Czech Republic

E-mail: Martin.Cernak1@vut.cz

Abstract. The aim of this study is to minimize minor losses in cap-end ports of a pneumatic cylinder used in pneumobil vehicle engine. Six geometry arrangements of intake ports, including the currently used version, were designed assuming conventional machining technology. Boundary conditions for the analysis were acquired from experimental measurement. The air flow was analyzed by 3D stationary CFD analysis in ANSYS Fluent for all designs. Pressure drop was used as the evaluation criteria. Two best configurations according to the obtained results were optimized using ANSYS Fluent Adjoint Solver. The pressure drop was reduced by 81.1% using this method. The obtained results will be used for design of solid geometry customized for production by lost wax casting process.

1. Introduction

Pneumobil is a racing vehicle powered by compressed air. These vehicles are designed and constructed by student teams for the *Emerson International AVENTICS^{TM} Pneumobile Competition*. Since 2012 *Pneumobil Racing Team Brno* has also been participating in this competition. In order to increase the power of the engine with double acting pneumatic cylinder, the cap-end and rod-end were customized. The pressurized air flows into and out of the cylinder through the cap-end and rod-end, respectively (Figure 1.(A),(C)). A second inlet port has been added and this adjustment has contributed to better acceleration and higher maximum speed. However, when designing these parts, no analysis has been used. Although the performance has been improved using customized end-ports, an engineering approach with the use of numerical analyses could provide an optimal geometry with a significantly better performance.

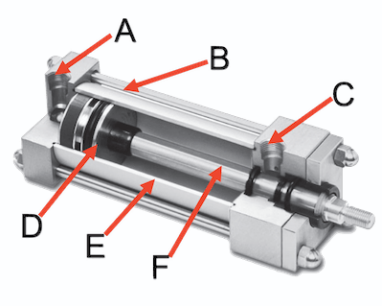

Figure 1. Section cut of double acting pneumatic cylinder; (A) cap-end; (B) tie rod;(C) rod-end; (D) piston; (E) barrel; (F) piston rod. [1]

Configuration of the inlet ports and their shape can cause boundary layer separation and thus a pressure drop, which is undesirable. Losses can be calculated analytically or empirically [2] for simple geometry configurations of internal fluid flow, typically consisting of sudden changes in diameter or change in flow direction. More complex flow configurations must be solved by Computational Fluid Dynamics (CFD). Fluid flow can be divided into laminar and turbulent, which is reflected also in the approach of the CFD solution. The most common way of solving turbulent fluid flow is using Reynolds-averaged Navier-Stokes equations (RANS). To solve the RANS equations it is necessary to choose an appropriate turbulence model completing the system of equations. There are many of these models, but the most frequently used are the k-ϵ and k-ω families. According to Bardina et al. [3] the SST k-ω turbulence model combines the advantages of both k-ϵ (activated far from a wall) and k-ω (activated near the wall) turbulence models and can be used for internal flow modeling [4, 5, 6].

A very effective tool for shape optimization is the Adjoint optimization method, which can be used for both internal and external fluid flow optimization. This method is very popular because of it's efficiency from a computational point of view, compared to other optimization methods such as the finite difference gradient based method or methods based on genetic algorithms [7]. The adjoint method can principally be divided into 3 main steps:

(i) solution of RANS equations describing fluid flow
(ii) sensitivity analysis of geometry according to observed objective variable (e.g. pressure drop)
(iii) change of fluid domain based on sensitivity analysis

These steps continue in an iterative manner until an optimal solution or a desirable design change is reached.

There are several studies dealing with this type of optimization, used for internal flow, that show a significant increase in overall flow performance. Lee et al. [5] have optimized a S-shaped duct which delivers air into a compressor of an aircraft engine using their own developed code. They have used SST k-ω turbulence model and results of pressure distribution have correlated well with the experimental data from the Aircraft Research Association. Results from Adjoint optimization have showed 1.5 % increase in total pressure recovery and decrease in flow distortion by 3-7 %. Horová et al. [8] have optimized flow in a water-glycol intercooler filling line, to minimize pressure drop. For this purpose ANSYS Fluent software has been used. Several turbulence models have been tried and finally the k-ϵ RNG with an enhanced wall treatment, has been chosen. During the solution there have been problems with convergence. These have been solved by a change in the dynamic viscosity. A pressure drop reduction by 23.9 % has been reached after recalculation with the correct value. Kim [9] et al. have optimized a U-bend of an internal cooling passage used in gas turbines. An adjoint method has been used for sensitivity calculations and geometry has been changed using topology optimization. An incompressible assumption has been used due to a Reynolds number of 100,000 and Mach number of 0.09. The final design of the U-bend has been compared using experimental measurement and a pressure loss reduction by 26.8 % has been achieved.

This paper presents a shape optimization of the cap-end used as an intake on a double acting pneumatic cylinder. The goal was to minimize the pressure drop by optimizing the location and angle of the air intakes, as well as the overall shape of the cap-end, using the ANSYS Fluent Adjoint Solver. This modification can lead to an increase in acceleration and top speed or to an improvement in maximum range of pneumobil vehicles.

2. Materials and Methods

2.1. Experimental measurement

An experimental measurement was performed to specify the boundary conditions for the simulation. A pneumatic scheme (Figure 2.) was designed to adhere to the competition rules

and the setup of the pneumatic circuit in the car. Pressure change at the pressure tank was measured assuming similar conditions as in the pneumatic cylinder. From this time dependence of pressure, mass flow rate was calculated using state equation and a constant temperature assumption $T = 20°$.

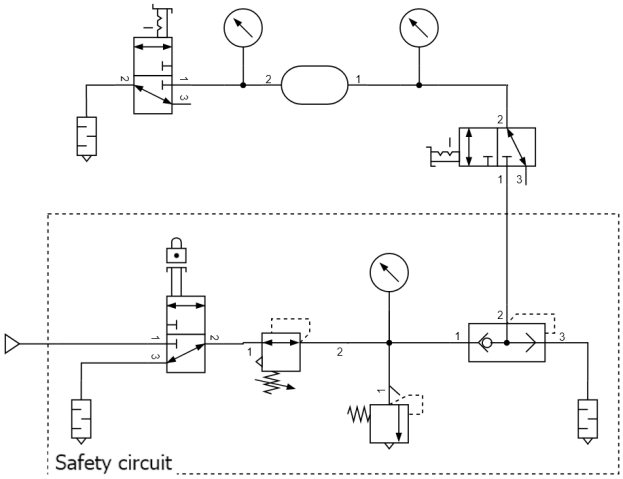

Figure 2. Pneumatic scheme of experimental measurement.

2.2. CFD analysis

To analyze the most suitable configuration of inlets, 3D stationary CFD analysis was performed in ANSYS Fluent. Six different geometries of the cap-end were designed (Figure 3.) assuming conventional machining technology. The rod-end was not analyzed nor optimized in this work. Fluid domain was extracted from these geometries and barrel with 100 mm diameter's volume was added (Figure 4.). The length of the barrel was set to 450 mm because of convergence issues caused by back-flow. Geometry A represents the current cap-end. Variants B and C have different depths of port drilling. The other configurations differ from each other by position and angle of the ports.

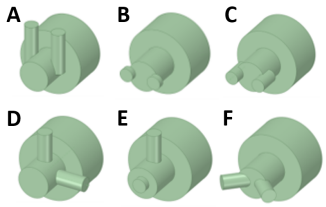

Figure 3. Proposed geometry configurations of end-cap.

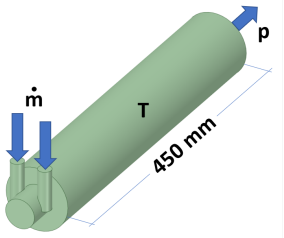

Figure 4. Fluid domain and applied boundary conditions.

The extracted domains were meshed using poly-hex core elements in Fluent Meshing. The discretized geometry was subsequently transferred to Fluent for solution. Air with ideal gas behavior was used as a fluid material. Energy equation was turned on. SST k-ω was chosen as a turbulent model. Boundary conditions were specified based on experimental measurement. Gauge pressure $p = 5$ bar at outlet and mass flow inlet $\dot{m} = 0.15$ kg $\cdot$ s^{-1} were used. Operating pressure was set to 101, 325 Pa. Constant temperature $T = 20$ °C was prescribed to walls, inlets and outlet (Figure 4.). Second order discretization schemes were used. An initial simulation was

performed to determine the flow character. The results showed an asymmetric flow (Figure 7.), so that simplification using a symmetry plane could not be used. Therefore, the full domain geometry was used for all models.

Reports of pressure at inlets and outlet and velocity magnitude at outlet were monitored simultaneously with residual convergence. Validity of obtained results was checked by mass flow balance and values of $y+$. Boundary cells were placed into log law region of wall function $y+ = 30$ to 300 in an iterative manner because of software license limitations. For this reason we can not claim that mesh independence was reached. However, the same meshing was used for all configurations and we suppose we were able to compare each other with sufficient precision. With this setup all 5 remaining domains were analyzed and 2 the best of them were optimized using Fluent Adjoint Solver as followed.

2.3. Shape optimization

Before the Adjoint optimization, 5 mm fillets were modeled at domain connections (Figure 5.) to reduce sudden change of diameters in geometry. The influence of these fillets on flow performance was tested and there was a significant reduction in pressure drop (see Results and Discussion). Therefore, modified geometries were further used and optimized.

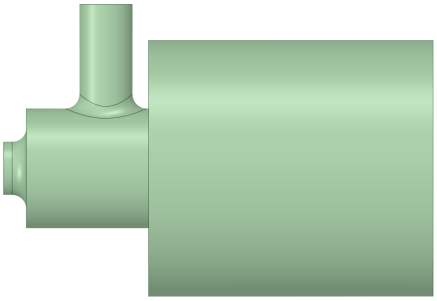

Figure 5. Modified fluid domain using fillets.

The pressure drop between inlets and outlet was chosen as an observed variable. For symmetric ports configuration, a pressure drop minimization of only 1 inlet was used as an objective. For asymmetric both of them was used. The best match of solution methods with analysis was used for Adjoint optimization. The only difference was in momentum, for which the first order upwind method was set. A stabilization scheme for the solution was enabled and adjoint residuals were set to 10^{-3}.

The polynomial morphing method was chosen for geometry change. A bounding box of end-cap was used in the design tool and the corresponding wall of flow domain was allowed to change (Figure 6.). Symmetry constraints were used. An adjoint calculation was conducted based on the flow analysis and the geometry was changed. This process ran in an iterative manner, until the change in observed pressure drop between two following iterations was less than 1 %.

3. Results and Discussion

3.1. Configuration of ports

The pathlines of the original geometry A are shown on Figure 7. There is a visible flow disorder induced by boundary layer separation in the barrel, causing a pressure drop. It can be seen that thr pathlines do not have symmetry behavior and the full model of geometry had to be used.

An analysis of velocity vector field at transversal plane of ports (Figure 8.) and at longitudinal mid-plane (Figure 9.), shows places which contribute to the pressure drop emerging in the end-cap. There could be seen places, typically near the sharp edges, where flow slows down and vortices are induced. For this reason fillets were added, before shape optimization.

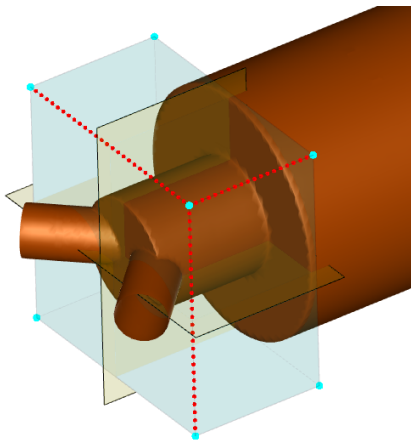

Figure 6. Bounding box and symmetry planes constraints.

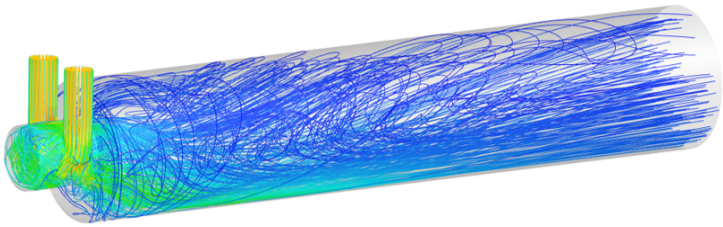

Figure 7. Flow characteristic of the currently used geometry.

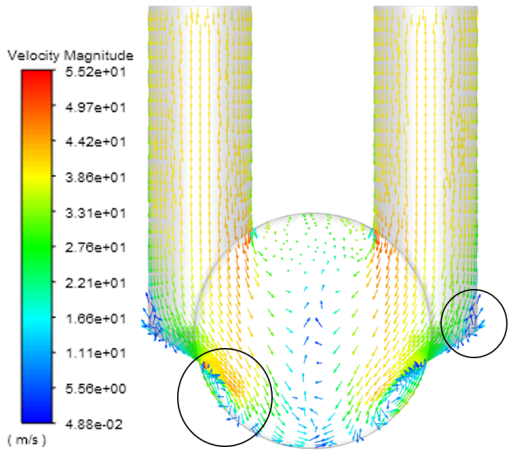

Figure 8. Transversal velocity vector field of geometry A.

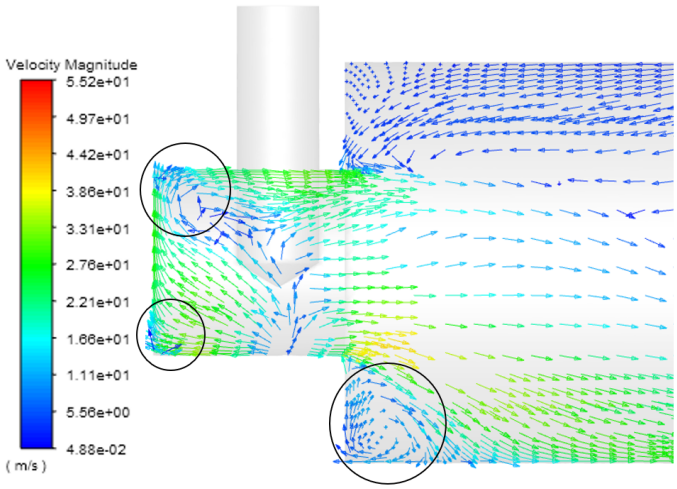

Figure 9. Longitudinal velocity vector field of geometry A.

The results obtained from the CFD analysis of all geometry configurations are summarized in Figure 10. The value of the pressure drop was calculated as a difference between average pressure of inlets and pressure at outlet, rounded to the nearest integer. The velocity vectors for the worst geometry configuration - B (Figure 11.), show massive back-flow reaching from barrel to the end-cap, resulting in the most significant losses. Other geometries differ up to 30 % and all of them have a lower pressure drop than the original geometry. The best two configurations, E and F, were redesigned with fillets and optimized.

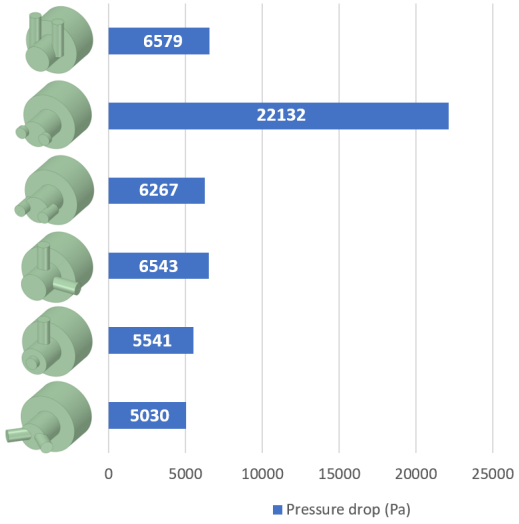

Figure 10. Results from analysis of various intake configurations.

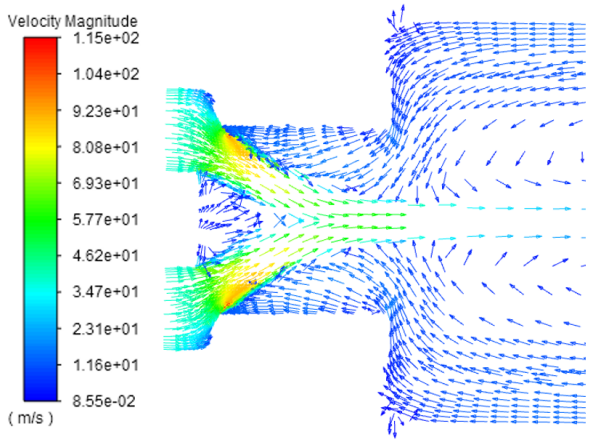

Figure 11. Velocity vector field for variant B

3.2. Shape optimization

The results obtained from the domain with fillets and following adjoint optimization, are concluded in Figure 12. and compared with unoptimized geometry. It can be seen that the geometry with fillets caused a pressure drop reduction to almost half of the original value. In the case of adjoint optimization, these values dropped by 67.1 % for geometry E and by 75.2 % for geometry F, from their original value. Final results were reached after 6 (E) and 7 (F) iterations. By combining change of port configuration and shape optimization, overall pressure drop makes up 18.9 % of current value. Optimized geometry of domain F is shown in Figure 13.

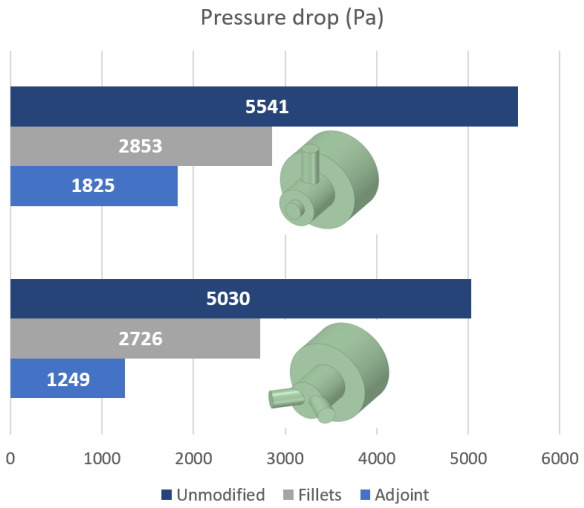

Figure 12. Results from shape optimization.

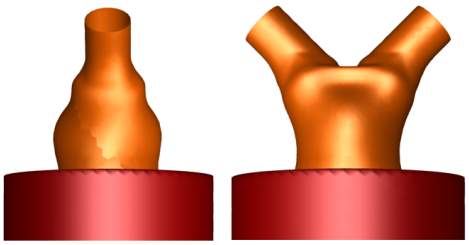

Figure 13. Optimized geometry of the best variant.

The velocity vectors of geometry F with fillets (Figure 14.(a)), show that vortices induced in the barrel are reduced, but those in the cap-end are still present (Figure 15.(a)). This situation is different for an optimized domain. Although boundary layer separation and vorticity can be seen in the barrel (Figure 14.(b)), vortices induced in the cap-end are smaller and closer to the wall (Figure 15.(b)), also velocity changes gradually from higher values at the inlets to lower at the barrel. The last two facts contribute to better flow performance, after adjoint shape optimization. Flow characteristics for geometry E are similar.

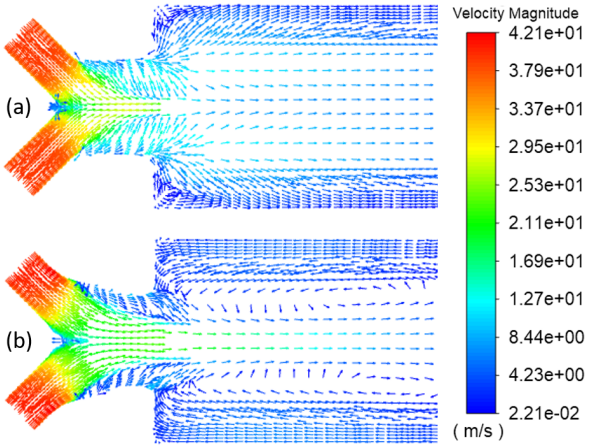

Figure 14. Longitudinal velocity vector field; (a) geometry with fillets (b) geometry optimized using adjoint method.

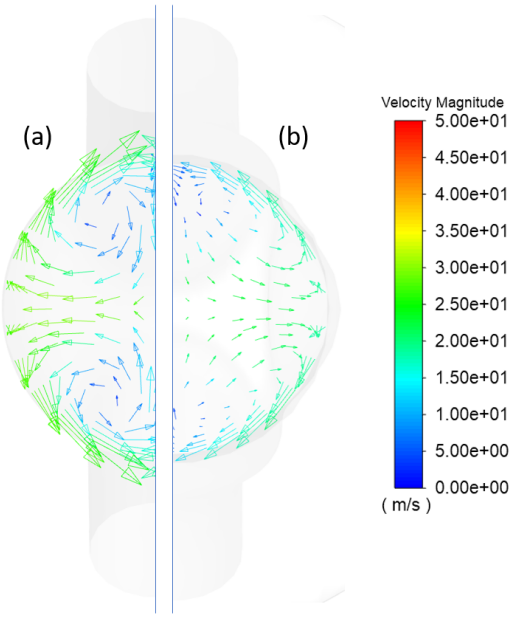

Figure 15. Transversal velocity vector field; (a) geometry with fillets (b) geometry optimized using adjoint method.

4. Conclusion

In this article, an optimization of fluid flow in the end-cap was performed, to reduce the pressure drop in the pneumatic cylinder used as an engine of the pneumobil vehicle. Based on the results obtained from 3D CFD analysis the two most suitable drafts of end-ports configuration, were chosen and further optimized, by means of ANSYS Fluent Adjoint Solver.

The obtained results, showed significant reduction of pressure drop, namely by 81.1 % for the best configuration, compared to currently used end-cap. The optimized part, will contribute to the performance improvement of pneumobile racing vehicles, resulting in higher maximum speed and longer range. Apart from the use in pneumobile vehicles, the obtained results can also be used for other specific applications of pneumatic cylinders. The follow up research will deal with the design of a solid geometry based on the obtained CFD results. The rod-end will also be optimized by the proposed workflow. These parts will be manufactured using lost wax casting and subsequently used and tested in the racing vehicle.

References

1. PNEUMATIC CYLINDER - HOW THEY WORK. *TAMESON* [online]. 2021 [visited on 2021-01-29]. Available from: `https://tameson.com/pneumatic-cylinders.html`.
2. MUNSON, B. R.; YOUNG, D. F.; OKIISHI, T. H.; HUEBSCH, W. W. *Fundamental of Fluids Mechanics*. 6th ed. New York: Wiley, 2009. ISBN 978-0470-26284-9.
3. BARDINA, J.; HUANG, P.; COAKLEY, T.; BARDINA, J.; HUANG, P.; COAKLEY, T. Turbulence modeling validation. In: *28th Fluid Dynamics Conference*. Reston, Virigina: American Institute of Aeronautics and Astronautics, 1997. Available from DOI: `10.2514/6.1997-2121`.
4. KIM, K.; LEE, Y. Design Optimization of Internal Cooling Passage with V-shaped Ribs. *Numerical Heat Transfer, Part A: Applications*. 2007, vol. 51, no. 11, pp. 1103–1118. ISSN 1040-7782. Available from DOI: `10.1080/10407780601112860`.
5. LEE, B. J.; KIM, C. Automated design methodology of turbulent internal flow using discrete adjoint formulation. *Aerospace Science and Technology*. 2007, vol. 11, no. 2-3, pp. 163–173. ISSN 12709638. Available from DOI: `10.1016/j.ast.2006.12.001`.
6. SCHMANDT, B.; HERWIG, H. Internal Flow Losses: A Fresh Look at Old Concepts. *Journal of Fluids Engineering*. 2011, vol. 133, no. 5. ISSN 0098-2202. Available from DOI: `10.1115/1.4003857`.
7. BREZILLON, J.; GAUGER, N. R. 2D and 3D aerodynamic shape optimisation using the adjoint approach. *Aerospace Science and Technology*. 2004, vol. 8, no. 8, pp. 715–727. ISSN 12709638. Available from DOI: `10.1016/j.ast.2004.07.006`.
8. HOROVÁ, Veronika; BOJKO, Marian; DOBEŠ, Josef. Methodology of using the Adjoint solver optimization tool during flow in the intercooler filling line to minimize pressure drop. *EPJ Web of Conferences*. 2019, vol. 213. ISSN 2100-014X. Available from DOI: `10.1051/epjconf/201921302025`.
9. KIM, C.; SON, C. Rapid design approach for U-bend of a turbine serpentine cooling passage. *Aerospace Science and Technology*. 2019, vol. 92, pp. 417–428. ISSN 12709638. Available from DOI: `10.1016/j.ast.2019.05.019`.